Structure and Stability of Networked Metallofullerenes of the Transition Metals

Manuel Sparta, Knut J. Børve, and Vidar R. Jensen*

Department of Chemistry, University of Bergen, Allégaten 41, N-5007 Bergen, Norway

Received: June 29, 2006; In Final Form: August 14, 2006

A DFT investigation of substitutionally doped fullerenes MC_{59} of second- and third-row transition metals shows that their stability increases toward the right-hand side of the d-block. Whereas the structural deviation from that of C_{60} depends on the size of the metal atom, stability is governed by electronic properties of the transition metal atom. A range of MC_{59} compounds of group 6−8 metals are predicted to have sufficient stability for experimental observation.

Introduction

Since the discovery of efficient means of mass-producing fullerenes, much effort has been spent on research on fullerene-based compounds with the hope that their particular electronic, optical and magnetic properties would lead to functionalized materials with a wide range of applications.[1−7] There are different ways to link a heteroatom to the fullerene structure, and most of the attention has been focused on endo- and exohedral binding modes, which leaves the carbon framework essentially intact. A more disruptive binding mode results from replacement of a carbon atom of the fullerene network by a dopant atom to obtain a substitutionally doped fullerene.[8] Substitutional binding opens for strong interaction between the dopant atom and the carbon network, involving both localized σ orbitals and delocalized π orbitals, making these compounds particularly interesting with respect to development of carbon nanomaterials with novel electronic properties such as long-range magnetic communication in carbon nanotubes.[9] Furthermore, the substitutional binding mode leaves the metal atom exposed to both the interior and the exterior of the carbon nanostructure, suggesting that these materials may, e.g., exhibit catalytic properties.[10]

Substitutional doping has been extensively explored for the elements immediately surrounding carbon in the periodic table, and synthetic routes to obtain macroscopic quantities of boron[11] and nitrogen[12] heterofullerenes have been devised. In contrast, evidence for substitutionally doped metallofullerenes has so far only been found in mass spectra following photofragmentation of metal−fullerene clusters in the gas phase,[13−16] or laser ablation of metal-graphite composites[10] or electrochemically deposited films of metal−fullerene clusters.[17] Among the early d-block metals, networked metallofullerenes, MC_n, have only been obtained in the case of Nb and La, and only for relatively small cages, e.g. up to $n = 50$ in the case of Nb. For the larger cages, the endohedral and exohedral structures dominate.[18,19] For the mid- and late-transition metals, the stability of the networked metallofullerenes seems to increase[10] and larger networked metallofullerenes such as MC_{59} have been observed for metals from group 8 (Fe[13,14]), 9 (Co,[13,14] Rh,[13−16] Ir[13,14,20]) and 10 (Ni,[13,14,16] Pt[16,20]).

Because of their difficult synthesis and metastable nature, knowledge about the structure and properties of the networked metallofullerenes is still scarce. Theory may complement the lack of experimental information. Density functional theory (DFT) has been applied in the study of all the above-mentioned networked metallofullerenes[15,17,20−24]in addition to other networked metallofullerenes.[25−27] Most of these works involve studies of the geometric and electronic structure of single substitutional metallofullerenes or comparison among a few of the experimentally observed compounds. The largest selection of metals is found in a local density functional investigation of the geometric and electronic structure of the networked metallofullerenes, MC_{59} (M = Fe, Co, Ni, and Rh).[22] Comparative studies of the relative stability of networked metallofullerenes for broad selections of metals, including metals that have not yet been observed to form such compounds, have not been reported.

Given the low stability of most of these compounds and the lack of insight into the factors governing their stability and properties, it is to be hoped that theory may contribute more directly to the synthesis of novel and potentially useful metal-doped carbon nanostructures by singling out target structures. We have thus embarked on a DFT-based screening of the structure of the monosubstituted Buckminster fullerene, MC_{59}, where the dopant atom (M) is varied systematically among the transition metals. It is our goal to establish direct relationships between the nature of the metal, the metal−fullerene bond, and the resulting stability of the metallofullerene. Preliminary results for the first-row transition metals have recently been reported.[28] Here, we report the corresponding results for the substitutional metallofullerenes of the second- and third-row transition metals and show that trends in bonding and stability for these compounds can be explained by a few atomic properties of the dopant metal atom. Furthermore, the present results for the second- and third-row transition metals are compared to those of the first row,[28] thus enabling us to address trends in geometric and electronic structure, bonding mechanism, and thermodynamic stability among substitutional metallofullerenes, MC_{59}, of all the group 3−10 transition metals. Particular attention is paid to properties that ensure strong metal−fullerene interaction and formation of stable metallofullerenes. Finally, we predict the future observation of a range of novel networked metallofullerenes whose stability should be sufficient for experimental detection.

* To whom correspondence should be addressed. E-mail: Vidar.Jensen@kj.uib.no. Telephone: (+47) 555 83489. Fax: (+47) 555 89490.

10.1021/jp064071h CCC: $33.50
Published on Web 09/26/2006

Computational Details

All calculations were performed using density functional theory (DFT) as implemented in the Gaussian 03 suite of programs.[29] Geometries of the Buckminster fullerene (C_{60}) and of the metallofullerenes (MC_{59}) were optimized within I_h and C_s symmetry, respectively, using analytic gradient techniques. The OLYP density functional, consisting of Handy's OPTX[30] modification of Becke's exchange and correlation due to Lee, Yang, and Parr[31] was applied in the geometry optimizations.

Carbon atoms were described by a Dunning and Hay double-ζ basis set ((9s,5p)/[4s,2p]) whereas for chlorine, a corresponding double-ζ plus polarization ((11s,7p,1d)/[6s,4p,1d]) basis set was used.[32,33] For the transition metals, the Stuttgart relativistic, small-core effective core potentials (ECPs) were applied, with cores of 28 and 60 electrons for the second- and third-row metals, respectively.[34] Valence electrons were described by the associated (8s,7p,6d)/[6s,5p,3d]-contracted basis sets.[34]

Total energies and properties were obtained in single point (SP) energy calculations in the optimized geometries using the three-parameter hybrid density functional method of Becke (termed "B3LYP"),[35] as implemented in the Gaussian 03 set of programs.[29] The SP calculations involved basis sets that were improved compared to those used in the geometry optimizations: The carbon and chlorine basis sets were extended by single diffuse p functions, and, in the case of carbon, also a single polarization d function.[33]

With the described method and basis sets for energy evaluation, the basis set superposition errors (BSSEs) of several of the $M-C_{59}$ complexes were found, using the counterpoise method, to be in the range 0.10−0.11 eV. In other words, the BSSE energies are small and relatively constant, and therefore the relative stabilities of the MC_{59} compounds are not affected to any significant extent and the BSSEs are not included in the current contribution.

All calculations were performed in an unrestricted formalism and the most stable spin state was located for each compound. The wave functions were routinely tested for spin and orbital instabilities and the expectation value of the $\hat{S}^2$ operator was computed to detect spin contamination. Whereas the solutions for some of the corresponding metallofullerenes of the first-row transition metals were found to be severely contaminated (contamination from next-higher-spin state higher than 5%),[28] and were corrected accordingly, none of the presently computed ground states were deemed to warrant correction.

Natural bond orbital (NBO[36]) analysis was used to characterize the electronic structure of the compounds. To quantify the degree of covalent bonding in the C−M bonds, we combine NBO electron populations and orbital characteristics into a bond-order index which depends linearly on the number of electrons in each of the natural bonding ($n_{\mathrm{occ},i}$) and antibonding ($n^*_{\mathrm{occ},j}$) orbitals as well as the amount of metal character in each of these orbitals ($f_{\mathrm{M},i}$ and $f^*_{\mathrm{M},j}$). Thus, each natural orbital that has either bonding or antibonding character between the metal M and a selected carbon atom contributes to the covalent bond order index, i.e.,

$$\mathrm{BO} = \sum_i n_{\mathrm{occ},i}\left(\frac{1}{2} - \left|f_{\mathrm{M},i} - \frac{1}{2}\right|\right) - \sum_j n^*_{\mathrm{occ},j}\left(\frac{1}{2} - \left|f^*_{\mathrm{M},j} - \frac{1}{2}\right|\right) \quad (1)$$

where i runs over all orbitals with bonding character between the metal M and the carbon atom in question and j runs over all the corresponding antibonding orbitals. The symmetry used in the calculations (C_s) does not formally exclude mixing of σ and π components. In practice, however, the σ and π bonds were found to be well separated in different natural bond orbitals and the summation over natural orbitals may thus be further resolved into σ and π components. The NBO calculations were performed using several different Lewis structures in order to assess the σ and π components.[37]

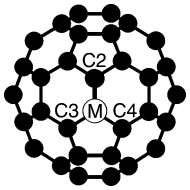

Figure 1. Labeling of the metal atom and its neighbors in the networked metallofullerenes, MC_{59}. Note that the M−C3 and M−C4 bonds are identical due to symmetry.

In this work, estimates of the thermodynamic stability of the substitutional metallofullerenes are obtained by using transition metal chloride salts as reference compounds. The stabilities are thus given as the energy of the reaction by which the metallofullerenes may be prepared from metal chlorides, chlorine gas, and C_{60}:

$$C_{60} + MCl_n + \frac{1}{2}(4-n)Cl_2 \rightarrow MC_{59} + CCl_4 \quad (2)$$

Trichlorides (i.e., $n = 3$) were used throughout except for group 10 for which the metals do not form stable trivalent compounds. We thus used dichlorides, i.e., $PdCl_2$ and $PtCl_2$, as reference compounds for group 10. It should be noted that transition metal trichlorides have, in fact, been used as starting material for formation of networked metallofullerenes via metal fullerides,[15] and we believe that the reference to common "off-the-shelf" chloride salts in eq 2 should provide a practical measure for the inherent stability of the monosubstituted metallofullerenes, MC_{59}. Where indicated, thermochemical values were computed within the harmonic-oscillator, rigid-rotor, and ideal-gas approximations.

Results and Discussion

For all transition metals, optimization of the metallofullerene compounds shows the existence of a stationary structure with the metal atom integrated into the fullerene cage by formation of bonds with the three neighboring carbons (labeled C2, C3, and C4, see Figure 1), resulting in the characteristic drop shape; see Figure 2.

The structural deviation from that of the unperturbed Buckminster fullerene depends to a large extent on the size of the metal, the larger atoms being shifted vertically upward relative to the smooth C_{60} surface: Whereas the latter has a small deviation from planarity[38] about each atom, $\Theta = 12.0°$, the MC_3 fragment of the large yttrium atom, for example, has a clear pyramidal character, $\Theta = 126.7°$, see Figure 2. On the other hand, least pyramidal character among the presently studied metallofullerenes is found for platinum ($\Theta = 85.9°$) and palladium ($\Theta = 89.3°$), rather than the slightly smaller elements in group 8 and 9 which nonetheless form shorter M−C bonds than do Pt and Pd, cf. Figure 2. Obviously, the degree of pyramidality depends not only on the radius of the metal atom, but also on its detailed electronic structure and the preference that the three-coordinate transition metal complex has for a pyramidal over a planar structure.[39−45]

Despite the severe distortions about the metal center seen particularly for the metallofullerenes of the larger metals, the

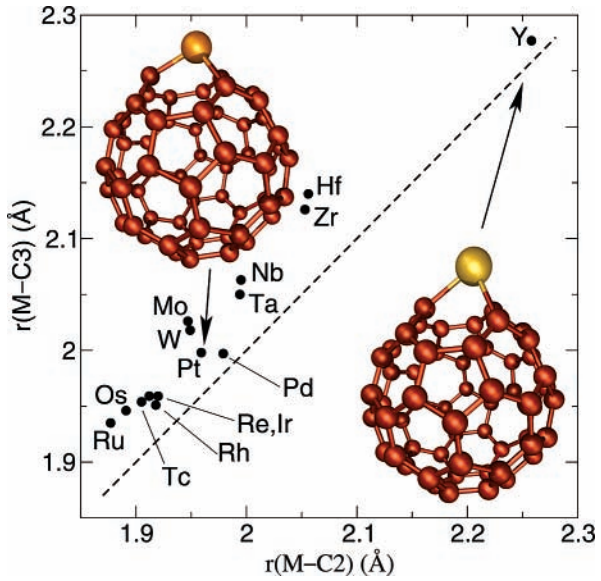

Figure 2. Metal−carbon bond distances, r(M−C2) and r(M−C3), of the networked metallofullerenes of the second and third row transition metals. See Figure 1 for atom labeling. Inserts: The molecular structure of the least (M = Pt, left, pyramidalization angle $\Theta = 85.9°$) and the most (M = Y, right, $\Theta = 126.7°$) pyramidal metallofullerenes. The pyramidalization angle, Θ, gives the departure from planarity.[38] Note that, due to the adopted view angle, the M−C3 bond eclipses the M−C4 bond.

perturbations caused by substitution do not propagate far into the carbon network. Outside the two six-membered and one five-membered rings joined by the metal atom, all C−C bond distances remain within 0.01 Å of those calculated for the Buckminster fullerene.

In fullerenes, bonds that are shared between two six-membered rings (often referred to as 6−6′ bonds) generally are found to be shorter than bonds at junctions between a six- and a five-membered ring (6−5 bonds), cf. Figure 1. This is particularly pronounced in C_{60}, for which $r(6-6') = 1.401$ Å and $r(6-5) = 1.458$ Å have been obtained by gas-phase electron diffraction.[46] Our corresponding computed bond distances, $r(6-6') = 1.411$ Å and $r(6-5) = 1.464$ Å, are in very good agreement with the experimental data. Similar to previous theoretical studies of selected metallofullerenes,[24,23] we find that this relationship between the bond distances, i.e., $r(6-6') < r(6-5)$, holds true also for bonds involving the metal, see Figure 2. In fact, the 6−6′ bonds are consistently shorter than the 6−5 bonds in all the networked metallofullerenes studied here.

Our calculated metal−carbon bonds for RhC_{59} (1.92−1.95 Å) are within 0.01 Å from those obtained using LDA (1.91−1.94)[22] and within 0.03 Å from the corresponding distances for three isomers of RhC_{53} computed using B3LYP (1.94−1.98 Å).[15] The calculated metal−carbon bond distances for PtC_{59} (1.96−2.00 Å) are found to be within 0.03 Å from the results obtained using LDA (1.93−1.99 Å),[17,20] and the corresponding agreement for IrC_{59}, 1.92−1.96 Å (this work) vs 1.91−1.95 Å,[20] is very good.

The calculated reaction energies according to eq 2 are all large and positive, implying that the substitutionally doped metallofullerenes are unstable with respect to formation of metal chloride salts, chlorine, and C_{60}; see Table 1. Furthermore, the reaction energy decreases to the right in each period, and thus at first glance the stability of the networked metallofullerenes seems to correlate with the amount of structural deformation following substitution. The smaller metals to the right appear

TABLE 1: Total Spin Expectation Values and Reaction Energies (eV) for the Formation of Metallofullerenes, MC_{59}, of the Second- and Third-Row Transition Metals, M[a]

	Y	Zr	Nb	Mo	Tc	Ru	Rh	Pd[c]
state[b]	$^2A'$	$^1A'$	$^2A'$	$^3A''$	$^2A''$	$^1A'$	$^2A'$	$^1A'$
$\langle \hat{S}^2 \rangle$	0.78	0.00	0.77	2.16	0.81	0.00	0.78	0.00
ΔE	9.40	7.62	6.44	5.30	4.50	2.84	2.34	2.91

	La	Hf	Ta	W	Re	Os	Ir	Pt[c]
state[b]		$^1A'$	$^2A'$	$^3A''$	$^2A''$	$^1A'$	$^2A'$	$^1A'$
$\langle \hat{S}^2 \rangle$		0.00	0.77	2.12	0.80	0.00	0.78	0.00
ΔE		7.68	6.43	5.12	4.05	2.40	1.86	2.22

[a] Reaction energies according to eq 2. [b] Molecular term symbol. [c] For metals of group 10, dichlorides are used as reference salts in eq 2 whereas trichlorides are used for all other groups.

to be significantly better integrated into the fullerene network than, for example, the large yttrium atom (cf. Figure 2), and one might expect the structural variation to manifest itself in the corresponding reaction energies of eq 2. The atomic radius of an element is of course intimately connected to electronic properties which in turn determine the nature and strength of chemical bonds, making it is difficult to separate electronic effects from those that may be attributed exclusively to atomic size. Important examples of the latter include structural deformation of the C_{59} network in order to accommodate the large heteroatom and nonoptimal C−M−C and C−C−M bond angles at the point of substitution. The second- and third-row transition elements are very similar in size, the radius of a given third-row metal normally being slightly larger than that of the second-row metal of the same group. Except for group 4, the metallofullerenes of the third-row transition elements are calculated to be more stable than those of the corresponding second-row transition elements, showing that pure size effects are not decisive for the stability of the networked metallofullerenes. This becomes even more evident when comparing with the smaller first-row transition elements.[28] Except for group 3 and 4, our calculated reaction energies for the metallofullerenes of the first-row transition elements are more positive than those of the second- and third-row transition elements. In group 8, for example, iron (covalent radius $r_{cov} = 1.17$ Å[47]) gives $\Delta E = 6.25$ eV for eq 2,[28] while the larger osmium ($r_{cov} = 1.26$ Å[47]) forms a considerably more stable metallofullerene, OsC_{59}, with $\Delta E = 2.40$ eV. Corrections to reach enthalpies and free energies are not expected to alter the trends formed by the relative energies to any significant extent. As a test we have calculated thermochemical corrections for the formation of RuC_{59}. At 298 K the reaction enthalpy is 2.75 eV, only 0.09 eV lower than the corresponding reaction energy ($\Delta E = 2.84$ eV). The reactions for formation of the present metallofullerenes are either identical (group 3−9) or very similar (group 10 compared to the other groups), except for the variation of the transition metal itself. Moreover, apart from some variations in shape and local geometry at the point of doping, the structure of the networked metallofullerenes are principally the same and contain identical numbers of metal−carbon and carbon−carbon bonds. In other words, in addition to being small, the enthalpic corrections are expected to be relatively constant among the present compounds. Because of the reduction in the number of particles in eq 2, the entropy correction is somewhat larger ($-T\Delta S = 0.42$ eV for RuC_{59}). However, all the formation reactions involve a reduction in the number of particles and the influence of entropy thus will also be fairly constant among the present compounds.

In addition to displaying a decreasing trend upon traversing each of the transition metal rows from left to right, the reaction

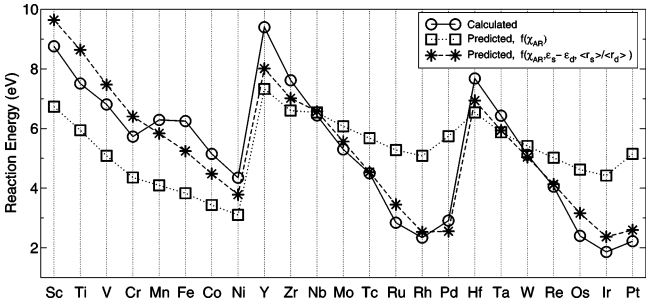

Figure 3. Predicted and calculated reaction energies for the formation of compounds MC_{59} according to eq 2. The linear regression models for prediction employ either only the electronegativity of the metal atom, to give the model termed $f(\chi_{AR})$, or the electronegativity, the energy splitting between *n*s and $(n-1)$d orbitals, and the relative size of the *n*s and $(n-1)$d orbitals, to give the model termed $f(\chi_{AR},\epsilon_s-\epsilon_d,\langle r_s\rangle/\langle r_d\rangle)$. See the text for details.

energies of eq 2 are increasing when descending groups 3 and 4 to the left and decreasing for the groups to the right; see Figure 3. As already noted, we believe that eq 2 represents a practical measure for the inherent stability of the networked metallofullerenes. Of course, a different choice of reference reaction would lead to different absolute values for the stabilities. However, it is gratifying that Ding et al.,[48] using a very different reference reaction, eq 3

$$C_{70} + M_2 \rightarrow MC_{69} + MC \qquad (3)$$

obtained calculated relative stabilities for metallofullerenes, MC_{69}, of group 9 transition metals in qualitative agreement with our stabilities for the corresponding compounds, MC_{59}, i.e., increasing metallofullerene stability upon descending the group is obtained in both studies. More importantly, this trend is observed in experiments.[14]

The above calculated and observed trends suggest that stability of the networked metallofullerenes could be connected to the "nobleness" of the metals, for example as measured by the ionization energy. Indeed, there is a clear negative correlation (correlation coefficient, $R^2 = 0.65$) between the first ionization potential and the reaction energy of eq 2 for all the three rows of transition metals. It is particularly notable that the vertical trend in stability, which changes from the early to the late transition metals, is discernible also for the first ionization energy of the transition metals. The ionization potential of the dopant metal atom was early singled out as important for obtaining the strong covalent metal−carbon bonds necessary for the realization of stable networked metallofullerenes.[10] Metals with low ionization potentials, on the other hand, tend to form endohedral metallofullerenes with predominantly ionic interactions between the encapsulated metal atom and the surrounding fullerene cage.[10]

The fact that covalent metal−carbon bonds seem to be important for obtaining networked metallofullerenes suggests that the electronegativity of the metal atom should be an even better indicator for metallofullerene stability than the ionization energy. In fact, the Pauling electronegativities of the three rows of transition metals are seen to correlate better ($R^2 = 0.81$) with stability than do the corresponding ionization potentials ($R^2 = 0.65$). However, there are severe problems connected to the Pauling electronegativities for the transition metals. For example, several of these electronegativities are higher than that of silicon, a metalloid, and in a thorough investigation of the Pauling scale the values for the transition metals have been characterized as "erratic and largely unrealistic".[49] Of the other electronegativity scales in common use, only the Allred−Rochow (AR) scale[50] is complete for the d-block. In contrast to the Pauling scale, AR electronegativities obey the "silicon-rule" and are not fitted to molecular data. In other words, they are strictly atomic, a fact which facilitates separation of the effects involved when using electronegativities to analyze chemical trends. The AR electronegativities were found to correlate surprisingly well ($R^2 = 0.92$) with metallofullerene stability for the first-row metals[28] and also describe the corresponding stabilities for the second- and third-row metals well ($R^2 = 0.85$), commensurate with the expectation that the late transition metals form stronger covalent bonds with the carbon network. However, for all the three rows together, the correlation is much less convincing ($R^2 = 0.26$), and thus vertical trends in metallofullerene stability are not well described by the AR electronegativities, see Figure 3. Vertical trends in transition metal chemistry are often related to the relative energies and spatial extensions of the metal valence s and d orbitals; see, e.g., refs 51−53. The 3d orbitals are relatively compact and low in energy compared to 4s and are less suitable for valence sd hybrid orbital formation than the 4d and 5d orbitals are. For example, the ratio between *n*s and $(n-1)$d radial expectation values is equal to 2.93 for iron and significantly lower for ruthenium and osmium (2.17 and 1.76, respectively).[54] We have tried to account for these effects by including the energy splitting between the *n*s and $(n-1)$d orbitals ($\epsilon_s - \epsilon_d$) as well as the ratio between the radial expectation values for the s and d orbitals, ($\langle r_s\rangle/\langle r_d\rangle$), as obtained from ref 54 in a three-variable linear model together with the AR electronegativity, χ_{AR}. The inclusion of the orbital descriptors drastically improves upon the model based on the AR electronegativity alone ($R^2 = 0.91$, as compared to $R^2 = 0.26$), indicating that the added parameters actually do handle the vertical variation as expected; see Figure 3.

Three metal−carbon σ bonds are found in all the metallofullerenes studied here and each of these bonds contain close to 67% metal $(n-1)$d. In other words, all the metal atoms are sd^2 hybridized. The easier hybridization predicted for the heavier elements (*vide supra*) manifests itself in higher σ bond orders. For example, the total σ bond order increases upon going from Ru (2.12) to Os (2.26), see Table 2, and both these elements, in turn, have a higher total σ bond order than that of Fe (1.91).[28] The fact that the d shell is becoming less compact and binds better with the valence orbitals of carbon upon descending the d block is also evident from the π bond orders, which are fairly constant among the rows for the early transition metals but increase markedly upon descending the groups 6−9. Again using group 8 as an example, the π bond order is seen to increase upon going from Ru (0.39) to Os (0.51), see Table 2, and both these elements in turn, have a higher total π bond order than that of Fe (0.34).[28]

The formation of better covalent bonds for the more electronegative metals to the right is reflected in the covalent bond orders (eq 1) given in Table 2. The σ bond orders increase steadily from left to right except for the last group (10), for which the metals prefer the +2 oxidation state and obtain somewhat lower bond orders than the neighboring metals to the left. It thus appears that the σ bond orders follow the trend formed by the stabilities and that, as indicated already by the correlation with properties such as the ionization potential and the electronegativity (*vide supra*), formation of covalent metal−carbon bonds is the main factor governing stability of the networked metallofullerenes. In fact, a linear model based on the σ bond orders is able to reproduce the stabilities with high accuracy for the second- and third-row metals ($R^2 = 0.91$) as

TABLE 2: Bond Distances (Å), Pyramidalization Angle (deg), and Covalent Bond Orders of Networked Metallofullerenes, MC_{59}, of the Second- and Third-Row Transition Metals, M[a]

	Y	Zr	Nb	Mo	Tc	Ru	Rh	Pd
r(M−C2)	2.26	2.06	2.00	1.95	1.91	1.88	1.92	1.98
r(M−C3)	2.28	2.14	2.06	2.03	1.95	1.93	1.95	2.00
Θ	126.7	112.1	106.3	102.8	96.4	93.7	94.2	89.3
BO_σ(M−C2)	0.30	0.51	0.59	0.64	0.68	0.70	0.73	0.64
BO_π(M−C2)		0.29	0.56	0.65	0.53	0.39	0.08	
BO_σ(M−C3)	0.32	0.51	0.57	0.64	0.68	0.71	0.76	0.68
BO_π(M−C3)		0.14	0.25	0.34				
BO_σ(total)	0.94	1.53	1.73	1.92	2.04	2.12	2.25	2.00
BO_π(total)	−	0.57	1.06	1.33	0.53	0.39	0.08	
BO(total)	0.94	2.10	2.79	3.25	2.57	2.51	2.33	2.00

	La	Hf	Ta	W	Re	Os	Ir	Pt
r(M−C2)		2.05	1.99	1.95	1.91	1.89	1.92	1.96
r(M−C3)		2.13	2.05	2.02	1.96	1.95	1.96	2.00
Θ		108.5	102.4	100.2	94.7	92.7	92.2	85.9
BO_σ(M−C2)		0.50	0.60	0.66	0.71	0.74	0.79	0.75
BO_π(M−C2)		0.25	0.50	0.66	0.59	0.51	0.10	
BO_σ(M−C3)		0.48	0.57	0.66	0.71	0.76	0.81	0.74
BO_π(M−C3)		0.13	0.27	0.43				
BO_σ(total)		1.46	1.74	1.98	2.13	2.26	2.41	2.23
BO_π(total)		0.51	1.04	1.52	0.59	0.51	0.10	−
BO(total)		1.97	2.78	3.50	2.72	2.77	2.51	2.23

[a] See Figure 1 for atom labeling. The M−C3 and M−C4 bonds are identical due to symmetry. The pyramidalization angle, Θ, gives the departure from planarity.[38] Bond orders, BO, are obtained using eq 1 and several different Lewis structures in the NBO calculations in order to assess the σ and π components.[37]

well as for all the three rows together ($R^2 = 0.88$). Equivalently, the trend in stability could be explained by the difference in hardness for the transition metals. The early metals are clearly hard acids and prefer the fairly hard chloride base in the reactants of eq 2 whereas the late metal ions studied here are borderline cases and prefer the softer fullerene fragment.

The π bond orders are smaller than their σ counterparts and are, of course, zero for the early metals, Sc and Y, which have all their valence electrons engaged in σ-bonds and also effectively zero for the group 10 metals which have more compact d orbitals and also prefer a low oxidation state (+2). The π bond orders vary smoothly along the rows from left to right, increasing at the beginning and reaching a maximum relatively early, in group 6, and decreasing to the right. The π bond orders thus do not correlate significantly with stability, suggesting that the π components of the metal−carbon bonds in the networked fullerenes do not translate into bond energy to the same extent as the σ components.

The increasing electronegativity of the metals through the rows is reflected in the decreasing polarity of the metal−carbon bonds; see Table 3. The NBO charges of group 3 and 4 second- and third-row transition metals are all above 1.5 e, whereas the corresponding charges for ruthenium and rhodium, for example, are below 0.5 e. It is remarkable that such a significant variation in metal atom charge is balanced almost exclusively by the charge of the neighboring carbon atoms, whereas the more distant C_{56} fragment absorbs a fairly constant amount of charge, $q_{C_{56}} = -0.38 \pm 0.12$ e. The lowest metal partial charges are found for ruthenium and osmium in group 8. Somewhat higher charges, in turn, are obtained for the late metals, in particular for the elements of group 10. The increased charge can probably be attributed to a lower electronegativity for the group 10 metals compared to the elements immediately to their left as well as to lower valency, i.e., reduced capacity for covalent bond formation compared to, e.g., the elements of group 8.

TABLE 3: NBO Partial Charges (e) Calculated for Networked Metallofullerenes, MC_{59}, of the Second- and Third-Row Transition Metals, M[a]

	Y	Zr	Nb	Mo	Tc	Ru	Rh	Pd
q_M	1.82	1.60	1.16	0.84	0.52	0.34	0.47	0.70
q_{C2}	−0.44	−0.52	−0.31	−0.20	0.02	0.07	−0.03	−0.20
$q_{C3} + q_{C4}$	−0.88	−0.79	−0.58	−0.35	−0.16	−0.02	0.01	−0.14
$q_{C_{56}}$[b]	−0.50	−0.29	−0.27	−0.29	−0.38	−0.39	−0.45	−0.36

	La	Hf	Ta	W	Re	Os	Ir	Pt
q_M		1.75	1.38	0.97	0.67	0.45	0.52	0.74
q_{C2}		−0.58	−0.40	−0.22	−0.04	0.03	0.00	−0.27
$q_{C3} + q_{C4}$		−0.91	−0.65	−0.42	−0.25	−0.07	−0.08	−0.17
$q_{C_{56}}$[b]		−0.26	−0.33	−0.33	−0.38	−0.41	−0.44	−0.30

[a] See Figure 1 for atom labeling. The C3 and C4 atomic charges are identical due to symmetry. [b] The combined charge on the C_{56} fragment of carbon atoms not directly bound to the metal.

Conclusion

We have shown that substitutionally doped metallofullerenes, MC_{59}, of second- and third-row transition metals are in general metastable with respect to formation of the transition metal trichloride (dichloride in the case of group 10 metals), chlorine gas, and C_{60}. However, the stability of these compounds generally improves toward the right-hand side of the d-block. Most of this improvement can be attributed to the increasing electronegativity of the late transition metals and the stability of this class of substitutional metallofullerene thus follows well-known trends in stability of organometallic compounds in general. The more electronegative metals to the right form increasingly covalent and stronger bonds to the three neighboring carbon atoms of the fullerene. In contrast, the size of the metal atom is seen to have little or no influence on metallofullerene stability despite significant local distortion of the spherical fullerene geometry upon doping with larger d-block metals such as yttrium. A comparison to similar results for the corresponding metallofullerenes of the first-row transition metals[28] shows that the relative energy and extension of the transition metal *n*s and (n − 1)d orbitals have to be accounted for in order to explain the vertical trends in stability in the d-block, i.e., the group trends. The overlap between the metal d orbitals and the sp hybrid orbitals of the neighboring carbon atoms increases down the groups, with significant improvement in overlap occurring in particular upon going from first- to second-row metals. To date, substitutional metallofullerenes, MC_{59}, of iron as well as of all the group 9 and 10 transition metals except for palladium have been observed in mass spectrometric studies.[13−16] We have already predicted that, among the first-row metals, chromium should form a slightly more stable substitutional metallofullerene than that of iron.[28] The present calculations involving second- and third-row transition metals suggest that a range of corresponding compounds of palladium as well as of group 6−8 metals may be more stable than that of iron and thus observable in experiment. Particularly promising stability is obtained for the elements below iron, ruthenium and osmium, and future observation of RuC_{59} and OsC_{59} may thus be anticipated.

Acknowledgment. The Norwegian Research Council is gratefully acknowledged for financial support through the NANOMAT program (Grant No. 158538/431) and the Strategic University Program in Quantum Chemistry (Grant No. 154011/420) as well as for grants of computer time through the Norwegian High Performance Computing Consortium (NOTUR).

Supporting Information Available: Tables giving molecular term symbols and optimized Cartesian coordinates as well as total energies of all the networked metallofullerenes presented in this article. This material is available free of charge via the Internet at http://pubs.acs.org.

References and Notes

(1) Goldshleger, N. F. *Fullerene Sci. Techn.* **2001**, *9*, 255.

(2) Chen, J.; Wu, F. *Appl. Phys. A: Mater. Sci. Process.-Mater.* **2004**, *78*, 989.

(3) Bystrzejewski, M.; Huczko, A. *Przem. Chem.* **2005**, *84*, 92.

(4) Bosi, S.; Da Ros, T.; Spalluto, G.; Prato, M. *Eur. J. Med. Chem.* **2003**, *38*, 913.

(5) Li, W. Z.; Liang, C. H.; Xin, Q. *Chin. J. Catal.* **2004**, *25*, 839.

(6) Margadonna, S.; Prassides, K. *J. Solid State Chem.* **2002**, *168*, 639.

(7) Segura, J. L.; Martin, N.; Guldi, D. M. *Chem. Soc. Rev.* **2005**, *34*, 31.

(8) Hummelen, J. C.; Bellavia-Lund, C.; Wudl, F. In *Topics in Current Chemistry*; Hirsch, A., Ed.; Springer: Berlin and Heidelberg, Germany, 1999; Vol. 199, p 93.

(9) Ruiz, E.; Nunzi, F.; Alvarez, S. *Nano Lett.* **2006**, *6*, 380.

(10) Clemmer, D. E.; Hunter, J. M.; Shelimov, K. B.; Jarrold, M. F. *Nature* **1994**, *372*, 248.

(11) Muhr, H.-J.; Nesper, R.; Schmyder, B.; Kotz, R. *Chem. Phys. Lett.* **1996**, *249*, 399.

(12) Reuther, U.; Hirsch, A. *Carbon* **2000**, *38*, 1539.

(13) Billas, I. M. L.; Branz, W.; Malinowski, N.; Tast, F.; Heinebrodt, M.; Martin, T. P.; Massobrio, C.; Boero, M.; Parrinello, M. *Nanostruct. Mater.* **1999**, *12*, 1071.

(14) Branz, W.; Billas, I. M. L.; Malinowski, N.; Tast, F.; Heinebrodt, M.; Martin, T. P. *J. Chem. Phys.* **1998**, *109*, 3425.

(15) Kong, Q. Y.; Zhuang, J.; Xu, J.; Shen, Y. F.; Li, Y. F.; Zhao, L.; Cai, R. F. *J. Phys. Chem. A* **2003**, *107*, 3670.

(16) Kong, Q. Y.; Shen, Y. F.; Zhao, L.; Zhuang, J.; Qian, S. X.; Li, Y. F.; Lin, Y. H.; Cai, R. F. *J. Chem. Phys.* **2002**, *116*, 128.

(17) Hayashi, A.; Xie, Y. M.; Poblet, J. M.; Campanera, J. M.; Lebrilla, C. B.; Balch, A. L. *J. Phys. Chem. A* **2004**, *108*, 2192.

(18) Tast, F.; Malinowski, N.; Frank, S.; Heinebrodt, M.; Billas, I. M. L.; Martin, T. P. *Phys. Rev. Lett.* **1996**, *77*, 3529.

(19) Klingeler, R.; Bechthold, P. S.; Neeb, M.; Eberhardt, W. *J. Chem. Phys.* **2000**, *113*, 1420.

(20) Poblet, J. M.; Munoz, J.; Winkler, K.; Cancilla, M.; Hayashi, A.; Lebrilla, C. B.; Balch, A. L. *Chem. Commun.* **1999**, 493.

(21) Meng, C.; Zhang, H. X.; Ge, M. F.; Feng, J. K.; Tian, W. Q.; Sun, C. C. *Chem. Phys. Lett.* **1999**, *309*, 344.

(22) Ding, C. G.; Yang, J. L.; Cui, X. Y.; Chan, C. T. *J. Chem. Phys.* **1999**, *111*, 8481.

(23) Billas, I. M. L.; Massobrio, C.; Boero, M.; Parrinello, M.; Branz, W.; Tast, F.; Malinowski, N.; Heinebrodt, M.; Martin, T. P. *Comput. Mater. Sci.* **2000**, *17*, 191.

(24) Alemany, M. M. G.; Dieguez, O.; Rey, C.; Gallego, L. J. *J. Chem. Phys.* **2001**, *114*, 9371.

(25) Campanera, J. M.; Bo, C.; Balch, A. L.; Ferre, J.; Poblet, J. M. *Chem.—Eur. J.* **2005**, *11*, 2730.

(26) Simeon, T. M.; Yanov, I.; Leszczynski, J. *Int. J. Quantum Chem.* **2005**, *105*, 429.

(27) Lu, G. L.; Deng, K. M.; Wu, H. P.; Yang, J. L.; Wang, X. *J. Chem. Phys.* **2006**, *124*, 054305.

(28) Sparta, M.; Jensen, V. R.; Børve, K. J. *Fuller. Nanotub. Car. N.* **2006**, *14*, 269.

(29) Frisch, M. J.; Trucks, G. W.; Schlegel, H. B.; Scuseria, G. E.; Robb, M. A.; Cheeseman, J. R.; Montgomery, J. A., Jr.; Vreven, T.; Kudin, K. N.; Burant, J. C.; Millam, J. M.; Iyengar, S. S.; Tomasi, J.; Barone, V.; Mennucci, B.; Cossi, M.; Scalmani, G.; Rega, N.; Petersson, G. A.; Nakatsuji, H.; Hada, M.; Ehara, M.; Toyota, K.; Fukuda, R.; Hasegawa, J.; Ishida, M.; Nakajima, T.; Honda, Y.; Kitao, O.; Nakai, H.; Klene, M.; Li, X.; Knox, J. E.; Hratchian, H. P.; Cross, J. B.; Adamo, C.; Jaramillo, J.; Gomperts, R.; Stratmann, R. E.; Yazyev, O.; Austin, A. J.; Cammi, R.; Pomelli, C.; Ochterski, J. W.; Ayala, P. Y.; Morokuma, K.; Voth, G. A.; Salvador, P.; Dannenberg, J. J.; Zakrzewski, V. G.; Dapprich, S.; Daniels, A. D.; Strain, M. C.; Farkas, O.; Malick, D. K.; Rabuck, A. D.; Raghavachari, K.; Foresman, J. B.; Ortiz, J. V.; Cui, Q.; Baboul, A. G.; Cliord, S.; Cioslowski, J.; Stefanov, B. B.; Liu, G.; Liashenko, A.; Piskorz, P.; Komaromi, I.; Martin, R. L.; Fox, D. J.; Keith, T.; Al-Laham, M. A.; Peng, C. Y.; Nanayakkara, A.; Challacombe, M.; Gill, P. M. W.; Johnson, B.; Chen, W.; Wong, M. W.; Gonzalez, C.; Pople, J. A. *Gaussian 03*, revision c.02; Gaussian, Inc.: Wallingford, CT, 2004.

(30) Handy, N. C.; Cohen, A. J. *Mol. Phys.* **2001**, *99*, 403.

(31) Lee, C.; W.; Y.; G.; P. R. *Phys. Rev. B* **1988**, *37*, 785.

(32) Dunning, T. H. *J. Chem. Phys.* **1970**, *53*, 2823.

(33) Dunning, T. H., Jr.; Hay, P. J. In *Methods of Electronic Structure Theory*; Schaefer, H. F., III, Ed.; Modern Theoretical Chemistry Series; Plenum Press: New York, 1977.

(34) Andrae, D.; Haussermann, U.; Dolg, M.; Stoll, H.; Preuss, H. *Theor. Chem. Acc.* **1990**, *77*, 123.

(35) Becke, A. D. *J. Chem. Phys.* **1993**, *98*, 5648.

(36) Glendening, E. D.; Badenhoop, J. K.; Reed, A. E.; Carpenter, J. E.; Bohmann, J. A.; Morales, C. M.; Weinhold, F. *NBO 5.0*; Theoretical Chemistry Institute, University of Wisconsin: Madison, WI, 2001; http://www.chem.wisc.edu/~nbo5.

(37) Different reference Lewis structures were tried in the NBO analysis in order to assess the stability of the computed M−C π-bond orders. For M = Y, Pd, and Pt, the π-bond order of the M−C bonds was found to be effectively zero and a Lewis structure with three metal−carbon single bonds represents the best description of the metal attachment to the carbon network. This is also the structure arrived at by the NBO program when run in unsupervised mode. For metals of group 4−6, a reference Lewis structure with three metal−carbon double bonds was specified. Although the latter structure does not represent the optimal solution found by the NBO program, all the three bonds contain a significant π component and specification of this Lewis structure does not affect the corresponding σ-bond orders. Finally, for the metals of group 7−9, only the M−C2 bond was found to contain a significant π component and a reference Lewis structure with two metal−carbon single bonds and one double bond was thus specified for these metals.

(38) The pyramidalization angle, Θ, gives the departure from planarity as $\Theta = 360° - \angle C_2MC_3 - \angle C_3MC_4 - \angle C_4MC_2$. For C_{60}, $\Theta = 12.0°$.

(39) Lauher, J. W.; Hoffmann, R. *J. Am. Chem. Soc.* **1976**, *98*, 1729.

(40) Jolly, C. A.; Marynick, D. S. *J. Am. Chem. Soc.* **1989**, *111*, 7968.

(41) Jolly, C. A.; Marynick, D. S. *Inorg. Chem.* **1989**, *28*, 2893.

(42) Castonguay, L. A.; Rappé, A. K. *J. Am. Chem. Soc.* **1992**, *114*, 5832.

(43) Bierwagen, E. P.; Bercaw, J. E.; W. A. Goddard, I. *J. Am. Chem. Soc.* **1994**, *116*, 1481.

(44) Margl, P.; Deng, L. Q.; Ziegler, T. *Organometallics* **1998**, *17*, 933.

(45) Jensen, V. R.; Børve, K. J. *Organometallics* **2001**, *20*, 616.

(46) Hedberg, K.; Hedberg, L.; Bethune, D. S.; Brown, C. A.; Dorn, H. C.; Johnson, R. D.; Devries, M. *Science* **1991**, *254*, 410.

(47) Pauling, L. *J. Am. Chem. Soc.* **1947**, *69*, 542.

(48) Ding, C. G.; Yang, Y. L.; Han, R. S.; Wang, K. L. *Phys. Rev. A* **2001**, *64*, 43201.

(49) Murphy, L. R.; Meek, T. L.; Allred, A. L.; Allen, L. C. *J. Phys. Chem. A* **2000**, *104*, 5867.

(50) Allred, A. L.; Rochow, E. G. *J. Inorg. Nucl. Chem.* **1958**, *5*, 269.

(51) Blomberg, M. R. A.; Siegbahn, P. E. M.; Nagashima, U.; Wennerberg, J. *J. Am. Chem. Soc.* **1991**, *113*, 424.

(52) Deubel, D. V.; Ziegler, T. *Organometallics* **2002**, *21*, 1603.

(53) Frenking, G.; Fröhlich, N. *Chem. Rev.* **2000**, *100*, 717.

(54) Visscher, L.; Dyall, K. G. *At. Data Nucl. Data Tab.* **1997**, *67*, 207.